IJISET - International Journal of Innovative Science, Engineering & Technology, Vol. 8 Issue 8, August 2021
ISSN (Online) 2348 – 7968 | Impact Factor (2020) – 6.72
www.ijiset.com

# Effect of In Situ Stress and Elastic Parameters on Rock Integrity for Hydrocarbon Recovery in 'BADE' Field Niger Delta

**Abiodun M. Ajibade[1], Olubola Abiola[2], Pius A. Enikanselu[2], and M. T. Olowokere[2]**

[1] Department of Physical Science, Olusegun Agagu University of Science and Technology, Okitipupa, Ondo State, Nigeria

[2] Department of Applied Geophysics, Federal University of Technology, Akure, Ondo State, Nigeria.

***Corresponding author (e-mail alongebiodun@gmail.com)**

## Abstract

The aim of this study is to evaluate rock integrity over 1D Mechanical Earth Model and 3D space to avoid blind exploration of zone where there are no well logs and provide information on the inter-well spatial variation properties for fracture, faulting, and wellbore stability within the study area. The objectives are to determine the state of in-situ stress to which a rock is subjected in depth; measure the rock mechanical properties and characterize the potential drilling hazard in terms of stresses, pressure, weak and fracture zones as well as geomechanical properties. Six (6) wells log and seismic data were used for the analysis. Geostatistical approach was used to build in-situ stress magnitudes and rock mechanical parameters from empirical relationship between density and velocity along 3D structural grid. Estimated in-situ stresses, pore pressure, elastic parameters and rock strength were integrated with all available information from well logs to establish the mechanisms governing the rock integrity in the study area**.** These were treated as properties, upscaled and distributed along the 3D structural grid. The results showed that integrity of shale formation within study area is weak compared to the surrounding reservoir sand. Generated cross-plots enable the proper examination and showed that this formation strength is low and incompetent enough to withstand high stress.

**Keywords:** In-situ stress; geomechanical properties; Mechanical Earth Model; borehole deformation; rock integrity; Geostatistics.

## Introduction

The knowledge about the stress condition is very important to rock integrity study for instance in performing drilling activities and determining wellbore stability. Application of stress over a rock unit can either make rock to deform (strain) or return back to its original shape, volume or dimension depending on the rock properties. The amount of the applied stress provides information on the strain as either elastic or inelastic.

### Previous Works

There has been significant hydrocarbon production from deepwater reserves and different challenges such as wellbore instability have also been encountered while exploring and developing these reserves according to Olowokere and Ojo, (2008a, 2008b).

Some of the research works conducted on this study are:

Prediction of pore pressure and uncertainty, in the Gulf of Mexico using 3D probabilistic Mechanical Earth Model (MEM) that combined well data with seismic velocities by Colin *et al.,* 2006. A prediction of pore pressure and uncertainty were made by sampling the region of parameter space consistent with available well data.

Fidelis and Akaha (2016), evaluated Rock mechanical properties that are critical to wellbore stability, well design, fracking, sanding prediction and production planning in 3 wells in an Onshore Field, Eastern Niger Delta. The investigated depth showed that Wellbore breakouts were predominant in shales and weak shaly sandstones across the lithologic units. Wellbore Stability Evaluation of Mishrif Formation in southern Iraq was studied by Alkamil *et al.,* (2017). They reported that stuck pipe was identified as a major geomechanical problem in several wells. In their study, a 1-D mechanical earth model (MEM) of the Mishrif formation was compiled based on the stress on and the rock strength parameters of the formation. The model was used to assess the influence of borehole collapse and subsequent stuck pipe problems.

The ‘Bade’ Field is an onshore field situated in OML-124 and located within latitude 5°30N and longitude 6°00E to latitude 5°40N and longitude 6°20E in the Niger Delta (Figure 1). It covers an area of 300 Sq. Km. The Field location is highly fractured and highly compartmentalized, therefore the drilling path of a well has to cross a fault.

This study intends to probe into the possibility of using seismically derived horizon and velocity to study rock integrity over 1D Mechanical Earth Model to 3D space to provide information on the inter-well spatial variation on porosity, pore pressure, fracture, faulting, and wellbore stability within the study area. The objectives are to determine the state of in-

situ stress to which a rock is subjected in depth; measure the rock mechanical properties and characterize the potential drilling hazard in terms of stresses, pressure, weak and fracture zones as well as geomechanical properties.

## Materials and Method of Data Analysis

### Elastic Property Modelling

Rocks with elastic properties have the ability to deform elastically and return back to its original state after the applied force is removed.

Poisson's ratio ($\nu_{dyn}$), Young's Modulus(E), Shear Modulus(G), bulk and matrix/grain moduli ($k_b$ and $k_m$), bulk and grain compressibility ($C_b$ and $C_r$), and Biot's coefficient (α) are the elastic properties obtained from wireline logs using different empirical relationships.

They were determined from the sonic interval transit time (compressional and shear), and density logs.

### Poisson's Ratio

Shear interval transit times data was not available in all the wells for computation of elastic parameters, and the knowledge of density and sonic compressional logs is not enough for computation of relative elastic and formation strength parameters that are need for geomechanical study, So an alternative approach was used to indirectly determine sonic shear transit time by a correlation of another elastic constant, the Poisson's Ratio (ν), to the pseudo q factor obtained from the Acoustic log and Density log.

The pseudo q factor is described as fraction of the total porosity occupied by disseminated shale. Therefore, Poisson's Ratio has been related to the shaliness index (Dresser Atlas, 1982). The factor q is indicative of the producibility of reservoir rock (Dresser Atlas). Irrespective of the type of shale distribution, it is possible to derive a pseudo value from density log and acoustic log porosity estimate.

$$q = \frac{\Phi_S - \Phi_{den}}{\Phi_S} \quad \text{---------- 10}$$

Where q is the pseudo factor, $\Phi_S$ and $\Phi_{den}$ are the porosities estimated from acoustic log and density log respectively Wyllie *et al.*,1956).. Density porosity was derived from bulk density using the equation below:

$$\Phi_{den} = \frac{\rho_{ma} - \rho_b}{\rho_{ma} - \rho_{fl}} \quad \text{---------- 11}$$

where: $\rho_{ma}$= matrix density, $\rho_b$ = bulk density (read from the log) $\rho_f$ = average density of fluid

second). A sonic derived porosity curve is sometimes recorded with the interval transit time. This sonic porosity is derived from the acoustic log using the equation below:

$$\Phi_S = \frac{\Delta tlog - \Delta tma}{\Delta tf - \Delta tma} \quad \text{---------- 12}$$

where: $\Delta_{tlog}$= interval transit time from log, $\Delta t_{ma}$ = interval transit time of the matrix material, $\Delta t_f$ = interval transit time of saturating fluid. Then, Poisson's ratio is computed using this equation.

Poisson's ratio (ν) =0.125*q+0.27 ---------- 13

Equation above was substituted into equation below to estimate shear transit time (Δts)

$\nu_{dyn}$ = 0.5*($\Delta Ts^2$/ $\Delta Tc^2$-1)/( $\Delta Ts^2$ / $\Delta Tc^2$-1) ---------- 14

$\Delta ts = \sqrt{(\Delta Tc^2\ (\nu - 1)/(\nu - 0.5)}$ ---------- 15

Poisson's Ratio is a dimensionless parameter that measures the ratio between lateral strain and axial strain (Walls and Jack, 1994). The remaining elastic parameters were further estimated after computing the shear transit time. Shear modulus

- G =RHOB*1/($\Delta Ts^2$) *1.34*$10^{10}$ ----------16

***Dynamic Young's modulus***

Fjaet *et al*, (1992) defined young's modulus as the ratio of the extensional stress to the extensional strain, which explain rock ability to resists compression by unconfined stress, that is the measure of the rock stiffness, and this has to do with porosity of rocks, because high porosity rocks will show decrease in rock stiffness and which will eventually lower its Young's modulus Yu and Smith, 2011.

Young's modulus was calculated from equation proposed by the following authors (Gatens *et al.,* 1990; Schlumberger, 2008; Yu and Smith, 2011) of which depends on elastic waves velocities

$E_{dyn}$ = $2\rho V_s^2(1+\nu)$ or 2G (1+ $\nu$); ---------- 17

Bulk modulus ($K_b$) is described as the ratio of stress applied to a unit of overburden rock

to the amount of volume change in the overburden rocks. High $K_b$ is an indication of rock stiffness, showing that the rock does not experience much compression (incompressibility) even under high stress.

It can be explained as the measure of rock's oppose to change in volume. When it is related to porosity its decreases as porosity increases in the rock leading decrease in rock's resistance to change in volume especially in highly stiff rocks like carbonates (Fadhil S.K *et. al.*, 2016).

Bulk and grain moduli equation (18 and 19) was obtained in terms of elastic wave velocities or transit times and bulk density (ρb) following (Gatens, et al., 1990; Schlumberger, 2008; Yu and Smith, 2011).

$k_b$ =RHOB*(1/(ΔTc $^2$)-4/(3* ΔTs $^2$) *1.34*10$^{10}$ ----------18

$k_m$ = $K_S\rho_{ma}$3*(ΔTc $^2$) *(ΔTs $^2$))/(3*ΔTs $^2$-4* ΔTc $^2$) ----------19

$C_b$ = 1/ $k_b$ ; ---------- 20

- $C_r$ = 1/$k_m$ ; ---------- 21

Since interval transit time was used for calculating elastic properties, coefficient 1.34*10$^{10}$ was used to convert the properties to geomechnical parameters in psi units.

Where. $V_p$ = compressional wave velocity, $V_s$=shear wave velocity, coefficient a = 13464, (ΔTc) = compressional transit time (µs/ft), (ΔTs) = shear transit time (µs/ft), D is the true vertical depth of interest. ν = Poisson's ratio, $K_S$ 1000m, $\rho_{ma}$ =2.65 g/c$^3$m

**Biot's Coefficient**

Biot's constant **(Biot, 1941)** is defined as a parameter that describes the ability of the pore pressure in a rock to oppose stresses acting on overburden rock. Biot's coefficient helps in knowing how an effective stress is affected by pore pressure. It was computed in terms of bulk and grain modulus equation 22 and 23

α = 1-$k_b$/$k_m$, in terms of bulk and grain modulus ---------- 22

Biot Constant can be defined as elastic parameter that depends on porosity, permeability, clay content, grain to grain contact, grain strength, and overburden pressure of rocks or sediments. Thus, it decreases as overburden pressure increase (Schlemberger, 1989; Fjaer *et al.*, 1992).

Rock compressibility is strongly related to grain size, pore space, cementation and weight of the overburden as Biot's constant is related to the pore space compressibility.

Biot constant was further obtained in terms of Bulk Compressibility ($C_b$) and Rock Matrix Compressibility (Cr), (Crain and Holgate (2004).

$\alpha$ = 1- $C_r$ / $C_b$, in terms of compressibility ---------- 23

**Inelastic Property Modelling**

Rock strength parameter (Unconfined compressive strength (UCS), cohesive and tensile strengths), internal friction angle ($\phi$) and Fracture gradient ($F$) were estimated from well logs using empirical equations and observe the link with elastic moduli (Dynamic young and statics (E) in each lithology unit. These were empirically calibrated against dynamic young's modulus by different authors. Babatunde et al., (2017) proposed UCS equation for Niger Delta was used

(UCS) =0.3966E+1.1956 ---------- 24

Empirical relation between Unconfined compressive strength and cohesion established by Zhang et al., (2010) was used for parameters below

Cohesion($C_o$) = $\frac{\text{UCS}}{2}$ $\frac{\cos\varphi}{1-\sin\varphi}$ ; - ---------- 25

Tensile strength ($T_o$) = Cohesive*cos $\varphi$/(2-sin $\varphi$) ---------- 26

Friction angle was estimated using Plumb's correlation (1994) in relation to the formation porosity and volume of the clay. Coe-efficient internal friction angle **μi** of was later computed from Internal friction angle. μi is defined to describe the increase in strength of intact rock with pressure

Friction angle ($\varphi$) =26.5-37.4*(1-NPHI-ShVol)+62.1* (1-NPHI-ShVol)$^2$) --------- 27

Coe-ffients of friction angle = Tan $\varphi$

Where unconfined compressive strength (UCS), Cohesive strength and Tensile strength are in Mpa unit. Cohesion (psi/ft).

## Results and Discussion

### Rock Mechanical Parameters Results

### Elastic Parameters

Elastic property profiles revealed that Bulk (Kb) and dynamic young's ($E_{dyn}$) moduli, decrease within shale but increase within sand. While Grain (Km) modulus, Poisson's ratio

and Biot's coefficient increase within shale but decrease in reservoir sand. It showed the shale formation has high compressibility (ease deformation) than the sand reservoir

The observation is clearly seen from 2300m to 2600m depth for shale in all the AK's wells and laterally from 3D models Figure 5a. These implied that, sand is more brittle than shale within this study area due to low Poisson's ratio and high Young's modulus. This formation has low resistance to stress. Therefore, can easily be broken by impart of little stress.

The encountered low bulk and young moduli and high grain modulus and Poisson's ratio was due to high porosity within shale formation, making shale to be less stiff than expected (Figure 5b). Shale formation porosity ranges from 0.30-0.41.

The high value of Poisson's ratio is an indication that shale formation within the study wells is not consolidated. It showed that as Poisson's ratio increases, it caused Young, bulk and shear moduli decrease due to fluid presence within the shale formation. Figure 7 shows that the Poisson's ratio of reservoir sand ranges from 0.10-0.27, while shale formation ranges 0.24-0.40.

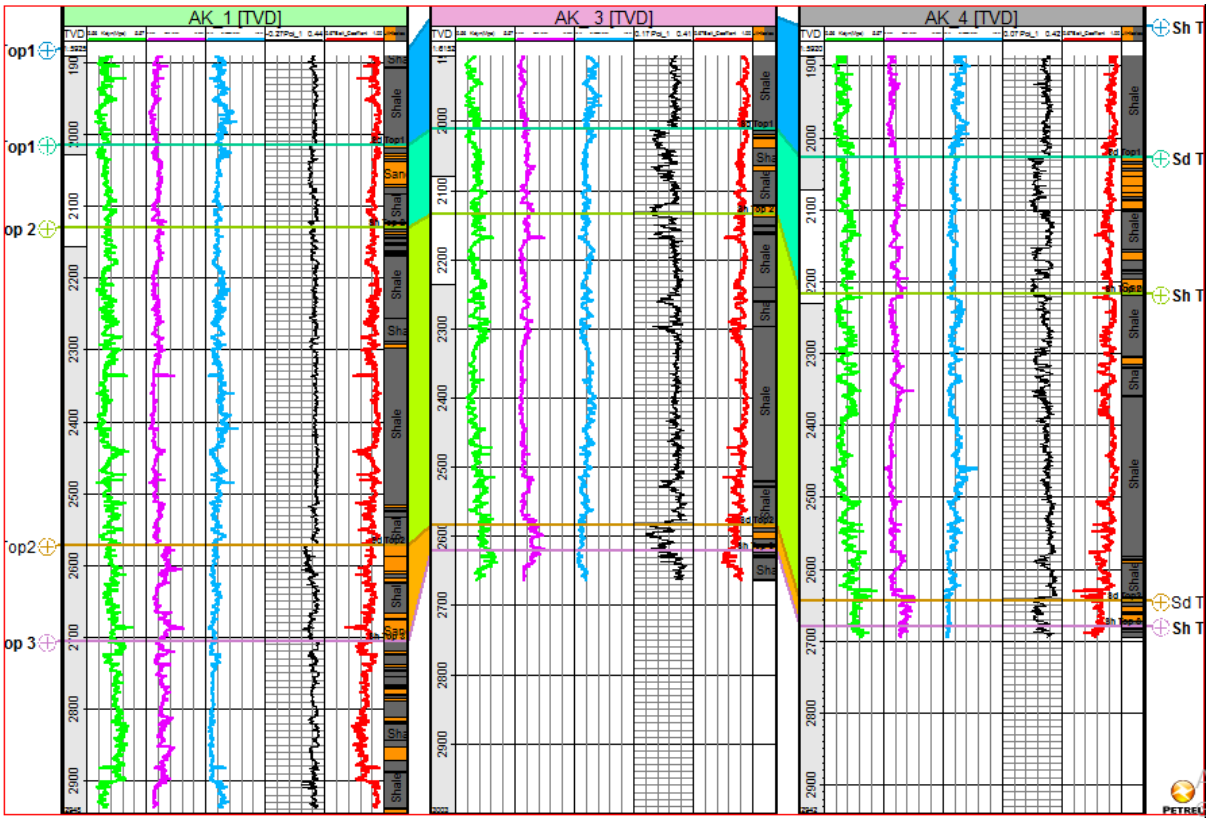


Fig 5a: Bulk, Young's, and grain moduli, Poisson's ratio, biot's constant, and litho-facies profiles.

IJISET - International Journal of Innovative Science, Engineering & Technology, Vol. 8 Issue 8, August 2021
ISSN (Online) 2348 – 7968 | Impact Factor (2020) – 6.72
www.ijiset.com

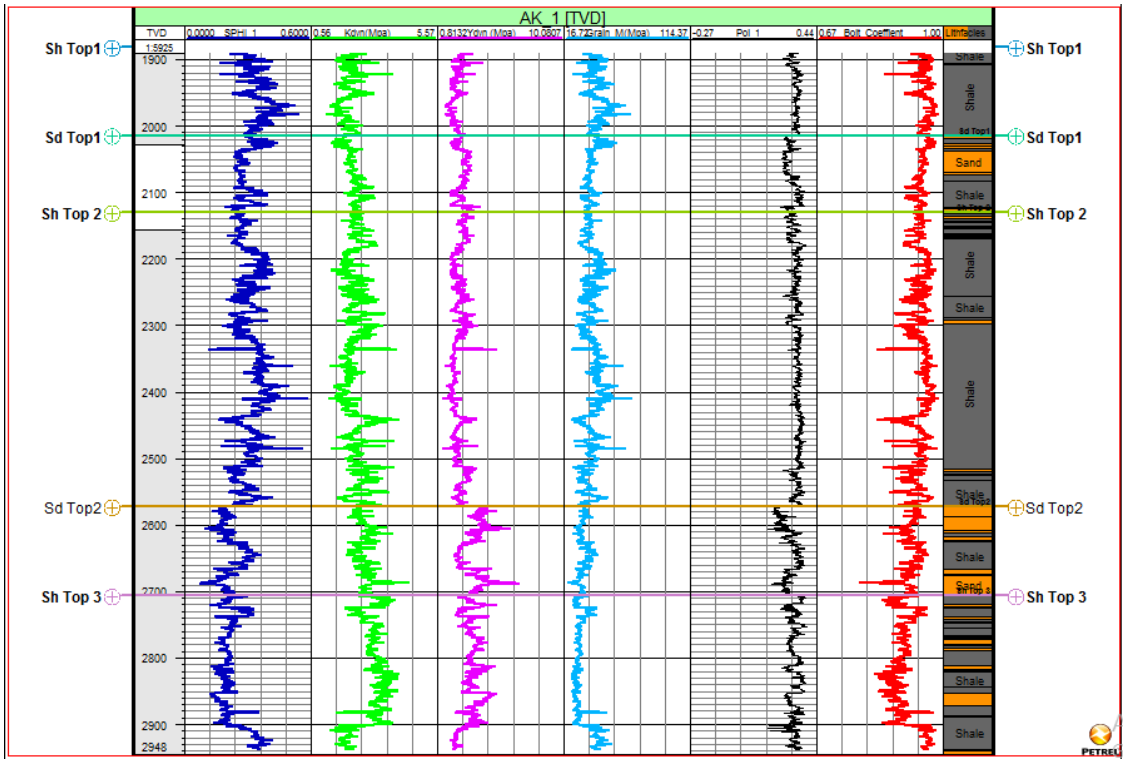


**Figure 5b:** Porosity, Bulk, Young's, and grain moduli, Poisson's ratio, biot's constant, and litho-facies profiles.

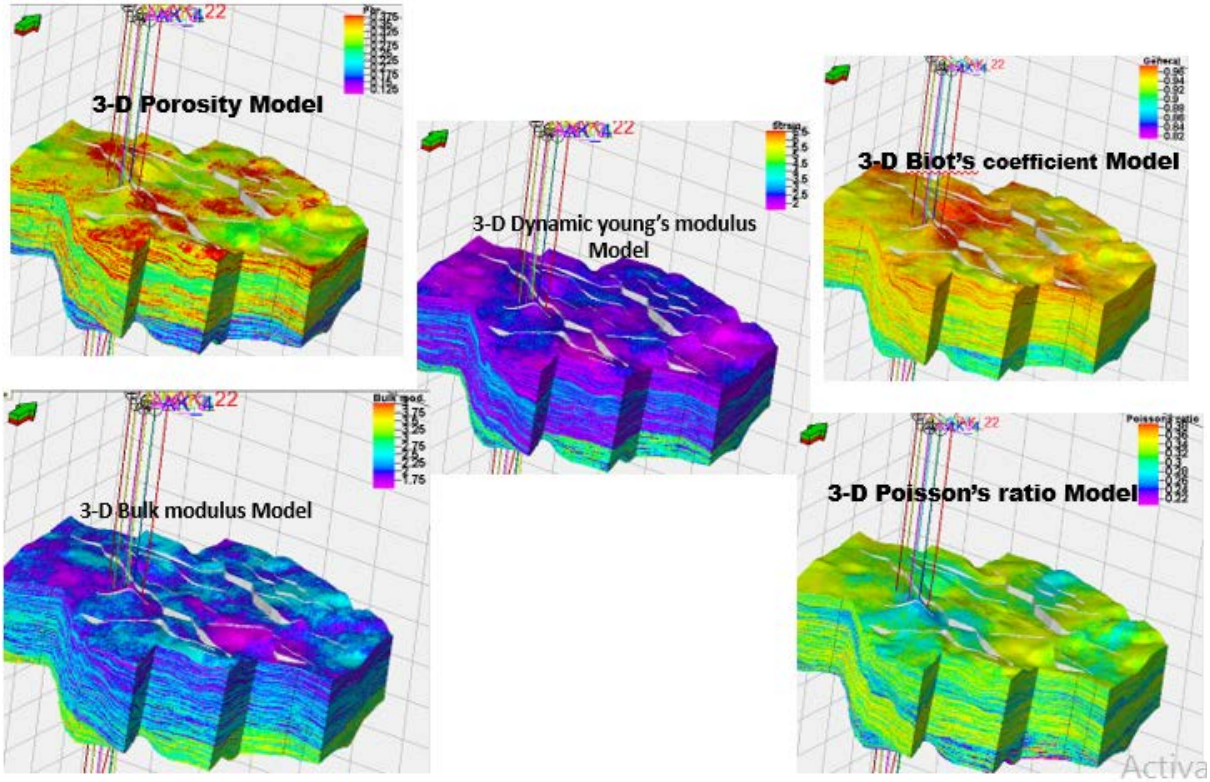


**Figure 6:** 3-D models for porosity, Bulk, grain, and Young's moduli, biot's constant, Poisson's ratio

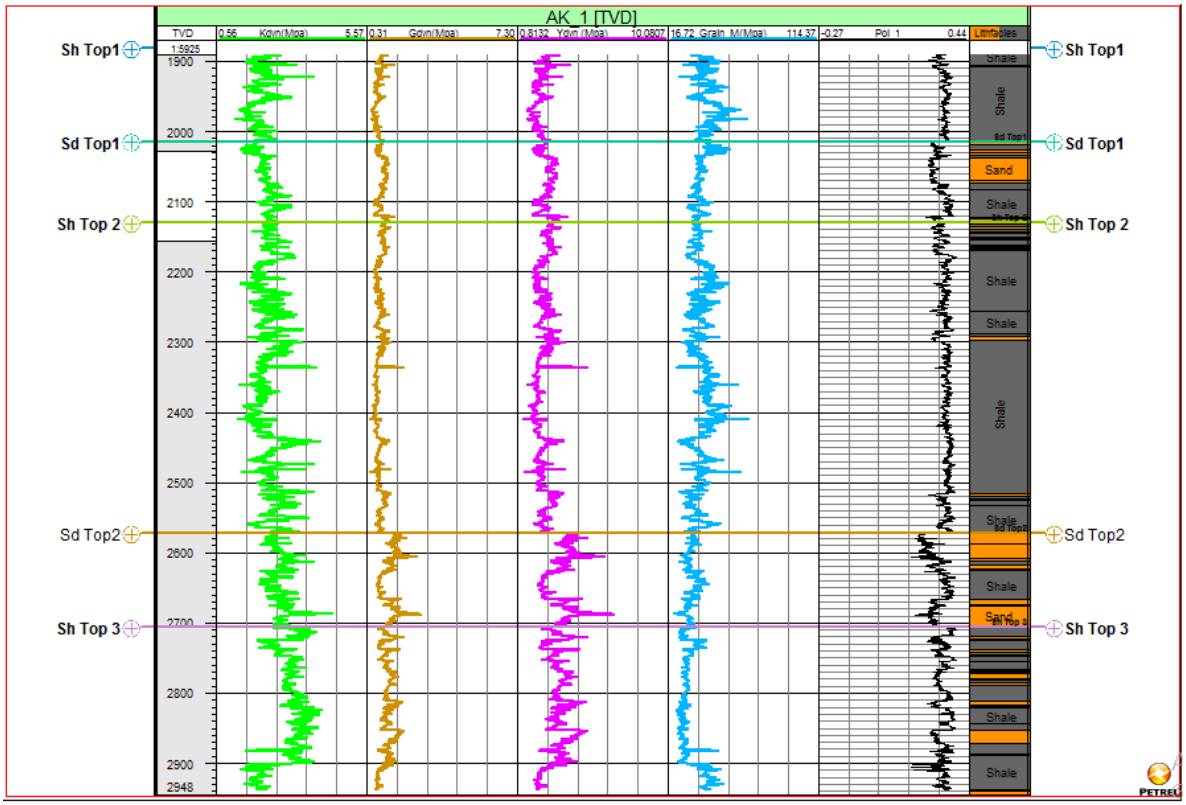


**Figure 7:** Bulk, Shear and Young's, grain moduli, Poisson's ratio and lithology profiles

1-D and 3-D view of Biot's constant and Pore Pressure models showed that Biot's constant decreases with respect to depth along the wellbore, due to porosity, permeability, clay content, grain to grain contact, grain strength, and overburden pressure (Figure 8). Meaning that as increase in overburden pressure caused biot's constant to decrease (Schlumberger, 1989; Fjaer *et al.*, 1992). The biot's constant decreases were as a result of high porosity and grain modulus leading to high compressibility of the formation. So, it has low resistance to oppose pore pressure. The results from the elastic were then used to determine shale formation and reservoir sand strength as either high or low (Figure 8).

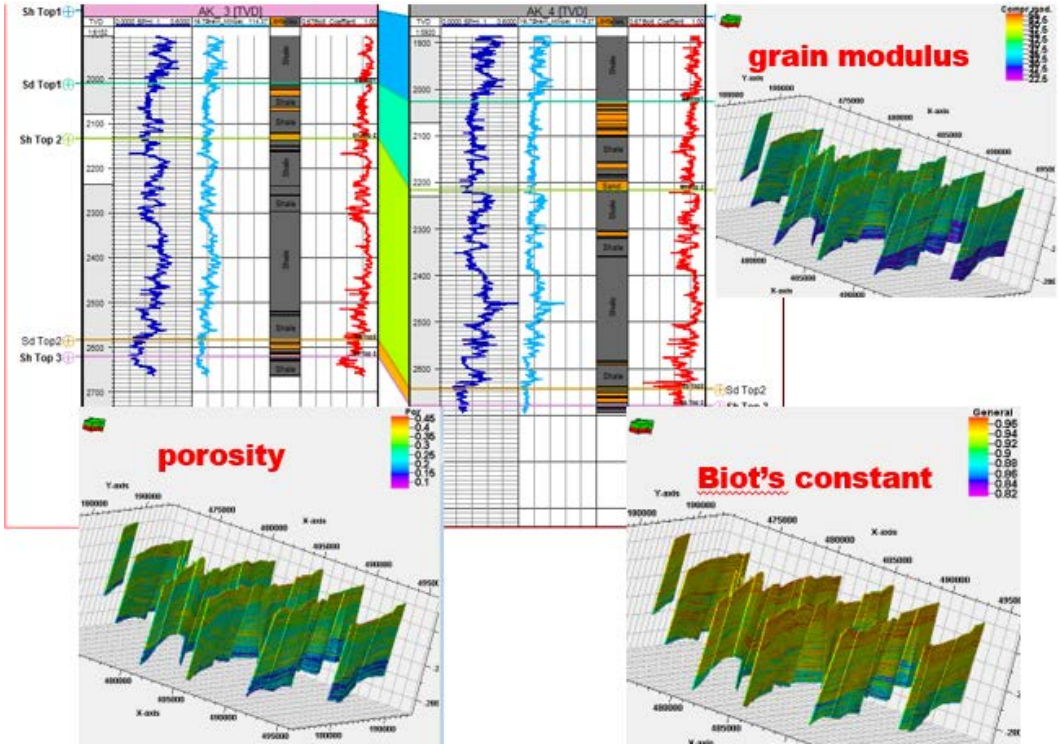


**Figure 8:** Porosity, Grain, modulus, litho-facies and biot's constant profiles

**Inelastic Parameters (Rock Strength Evaluation)**

Estimated Velocity, Tensile, Unconfined compressive strength (UCS), cohesive strength and internal friction angle showed that the shale formation is not strong (low values) along wellbore revealing weaker or lower strength. While reservoir sand showed higher strength. This can be observed for reservoir sand and shale formation thickness from 2316m to 2700m was considered for AK-1 and 2316.328-2663.952m for AK-3 (Figure 9). The observed low cohesive strength and internal friction angle within shale formation was due to nature and mineral contents of shale (high mica content) (Olowokere, 2010; Barton 1973; Jaeger and Cook 1976). The friction angle for shale formation ranges from $20^0$-$25^0$ while sand has higher values from $25^0$ and cohesive strength is high for reservoir sand Figure 9. Generated cross-plots from Young's modulus against velocity and cohesive strength against internal friction angle for AK-1 and AK-3, revealed that velocity decrease as young's modulus decrease within shale formation due to its low strength and less cohesiveness (Figure 10).

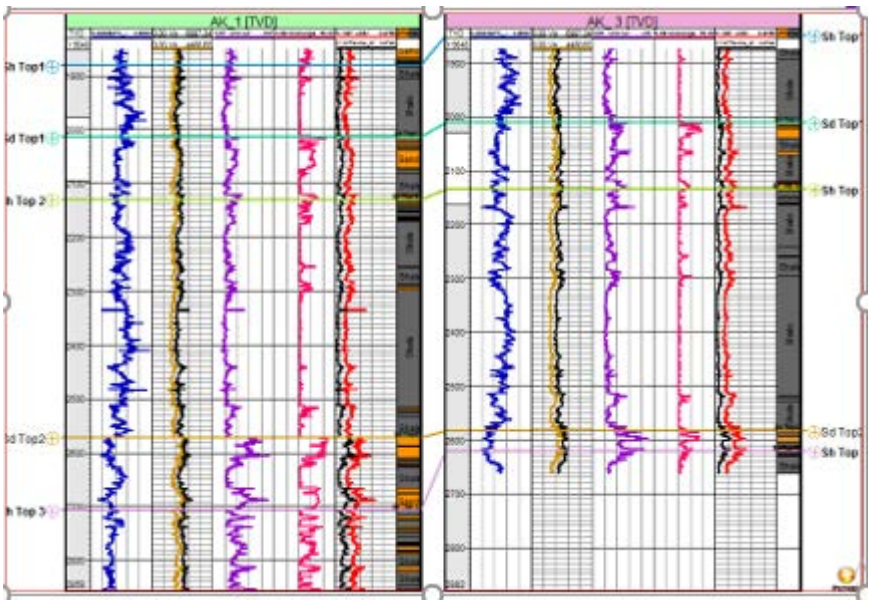


Figure 9a: Porosity, Compressive and shear velocities, Cohesion, internal Friction angle, Tensile and Unconfined compressive strength and lithology profiles

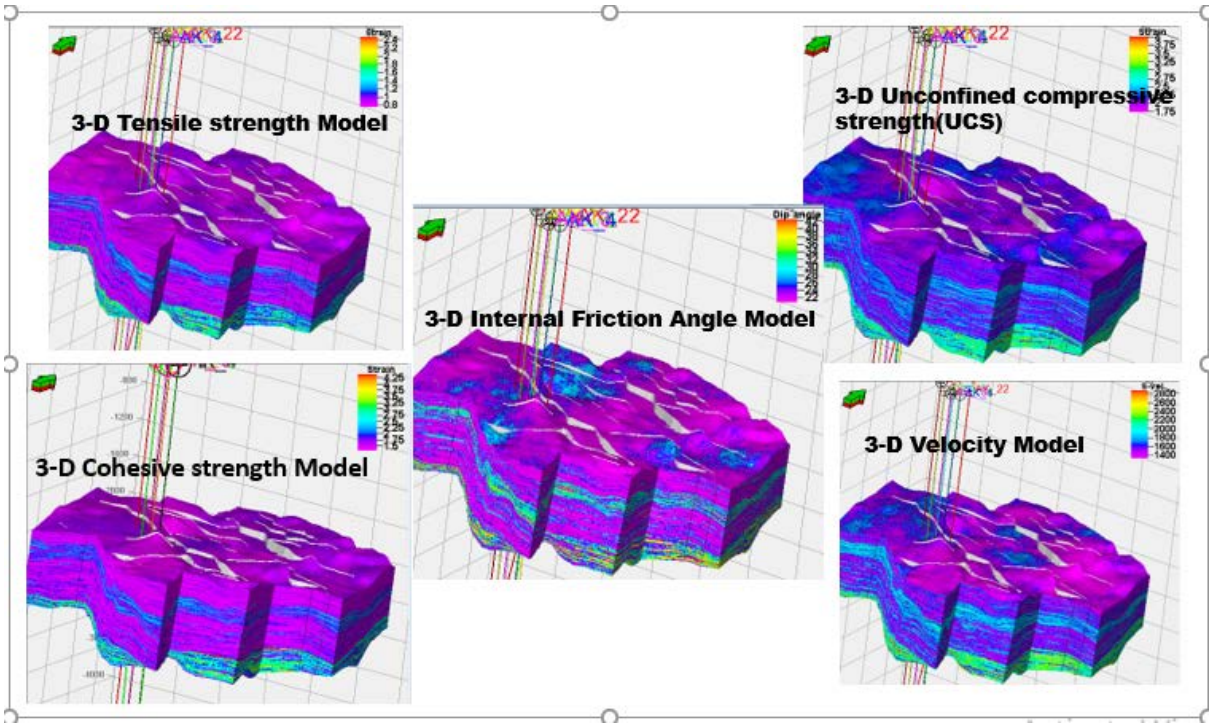


Figure 9b: Cohesive, Tensile and Unconfined compressive strengths, internal Friction angle, and velocity.

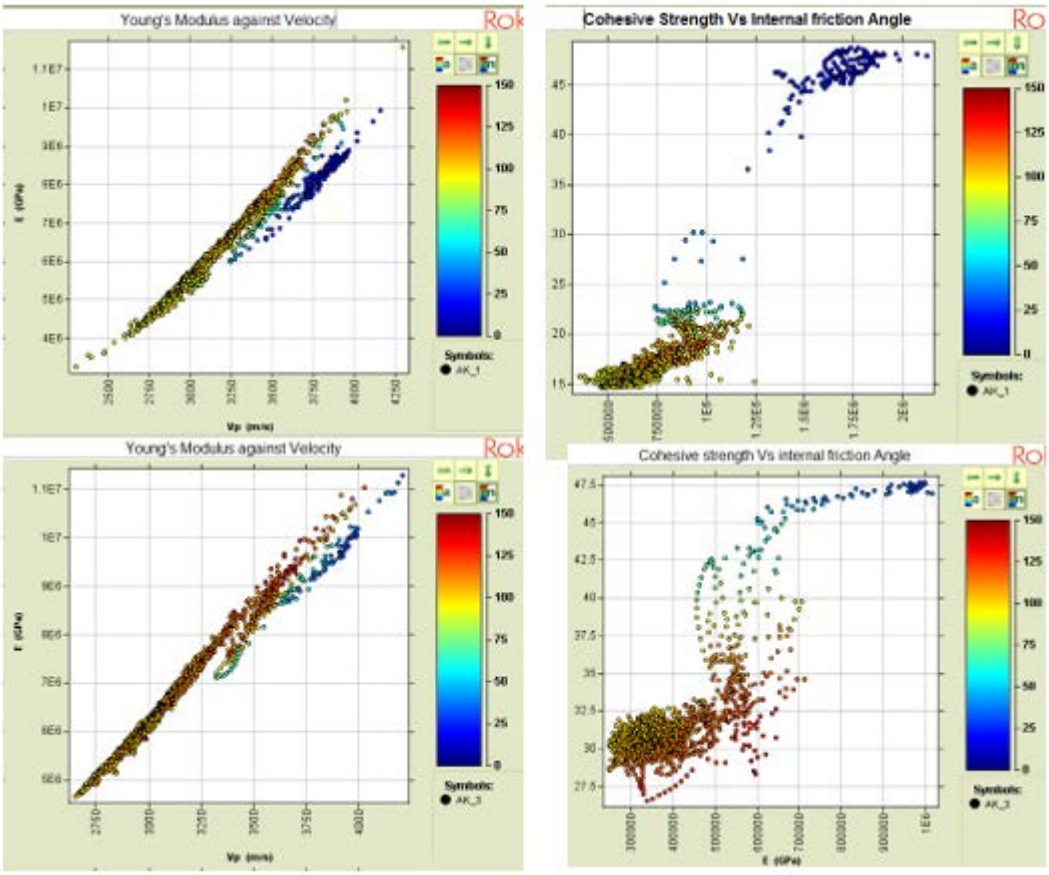


Figure 10: cross-plots of Young's modulus against velocity and Cohesive strength against internal Friction angle

**Potential Drilling Hazards Analysis**

Geophysical well logs, Pore Pressure, Stresses, as well as Geomechanical parameters were used to explained possibility of drilling hazards within the shale formation as a result of nature of the shale formation encountered within the study area. Figure 11 shows the Litho-facies, bulk and young's moduli, unconfined compressional and cohesive strength and stress (vertical, and max and mini horizontal) profiles for AK-1 and 3.

Ductility or Brittleness of Shale Formation was analysed and it showed that the Shale formation is brittle in nature due to the type of clay content, low elastic moduli and strength which had been affected greatly by high in-situ stress. The brittleness has given room for fractures due to either tectonic movement or during drilling operations (Taeyoun KIM *et al.*, (2016), Jaeger et al., 2009 and Yang *et al.*, 2013). The fractures coupled with higher in-situ stress anisotropy in the shale have significantly weakened its integrity (Fig. 11). This made rubble of the rock to fall into the hole, creating hole enlargement in some of the wells. These parameters were confirmed to be the same for other wells.

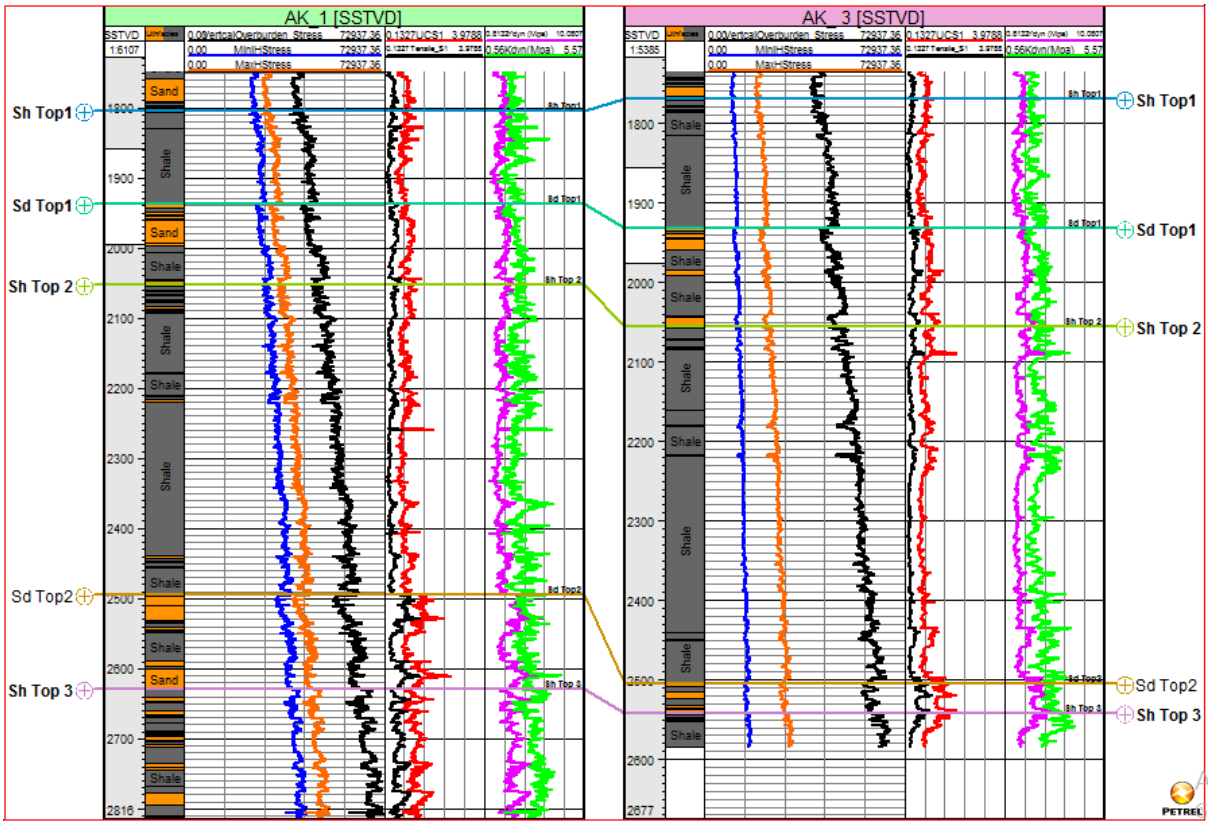


**Figure 11: Litho-facies, bulk and young's moduli, unconfined compressional and cohesive strength and stress (vertical, and max and mini horizontal) profiles for AK-1 and 3**

## Weak and Fracture Zones Analysis Results from Well Logs

The presence of weak and fracture formation was analysed from gamma, caliper and bit size, sonic and density porosity logs to detect wellbore problems (breakout, hole enlargement keyseats e.tc) within zones of interest.

### *Caliper and Bit Size Log Analysis*

Breakout or collapse was observed at different depth within shale formation from difference between bit size and caliper logs as a result weak sediments falling off or caving into wellbore, Figure 12.

Breakout zones depth interval is between 1913.14-2027.07m, 2215.05-2265.28m at AK-2, while 1943.90-2085.70m and 2237.71m-2517.04m at AK-6. There are present of breakout at AK-2 and AK-6, keyseat at AK-3 and AK-5, while washout is observed at AK-1. Hole diameter irregularity and enlargement was observed in shale formation in all the wells due to induced stress. Zoback,2003

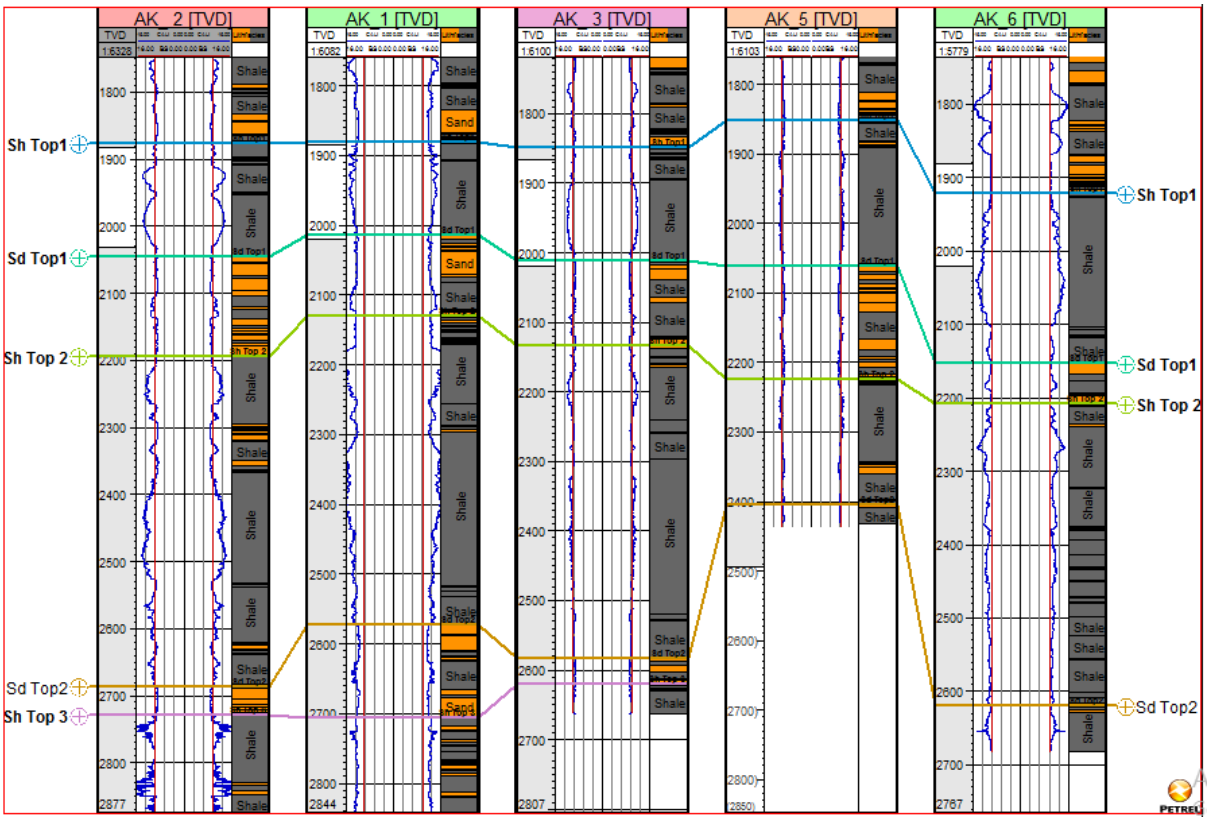


Figure 12: caliper, bit size and litho-facies logs for AK-2, 1,3, 5 and 6

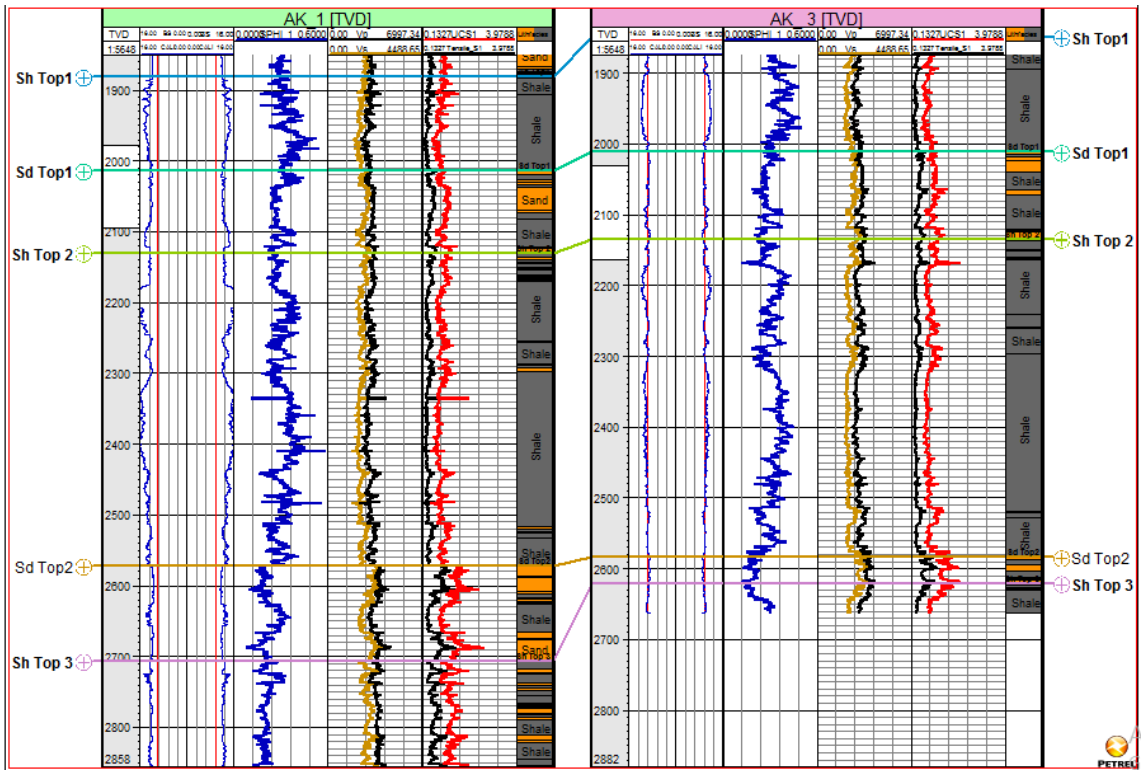


Figure 13: Caliper, bits size, vol. of shale, porosity, Compressive and shear velocities, Young's modulus Tensile and unconfined compressive strength profiles.

**Stresses, Pore Pressure and Geomechanical parameters**

These can be properly seen from the depth interval of 2316m-2600m (758.53ms-1039.53ms) as in-situ stress and pore pressure magnitudes increase in with respect to depth as well as reduction in elastic parameters and rock strength within shale formation of the study area, Figure 10. Crossplots of UCS against young modulus, porosity and velocity further confirmed that shale formation has lower strength (weaker than sand). That's this formation is not competent enough to withstand high stress impart Figure 16. Wherefore prone to be dangerous while drilling. Chang, *et al.*, (2006).

High in-situ stresses, pore pressure, low rock strength, and presence of micro-fractures within shale formation along wellbore and lateral view from the generated models confirmed the possibility of wellbore breakout or rock failure to occur within the study area, if further drilling practice is not properly carried out. Since, Wellbore breakout was observed in all Bade fields. Elastic, inelastic and stress explained observed brittle faulting of rock units from seismic section (Inline 400) and 3-D litho-facies model Figure 17 and wellbore breakout and hole enlargement in all AK" S Well along wellbore.

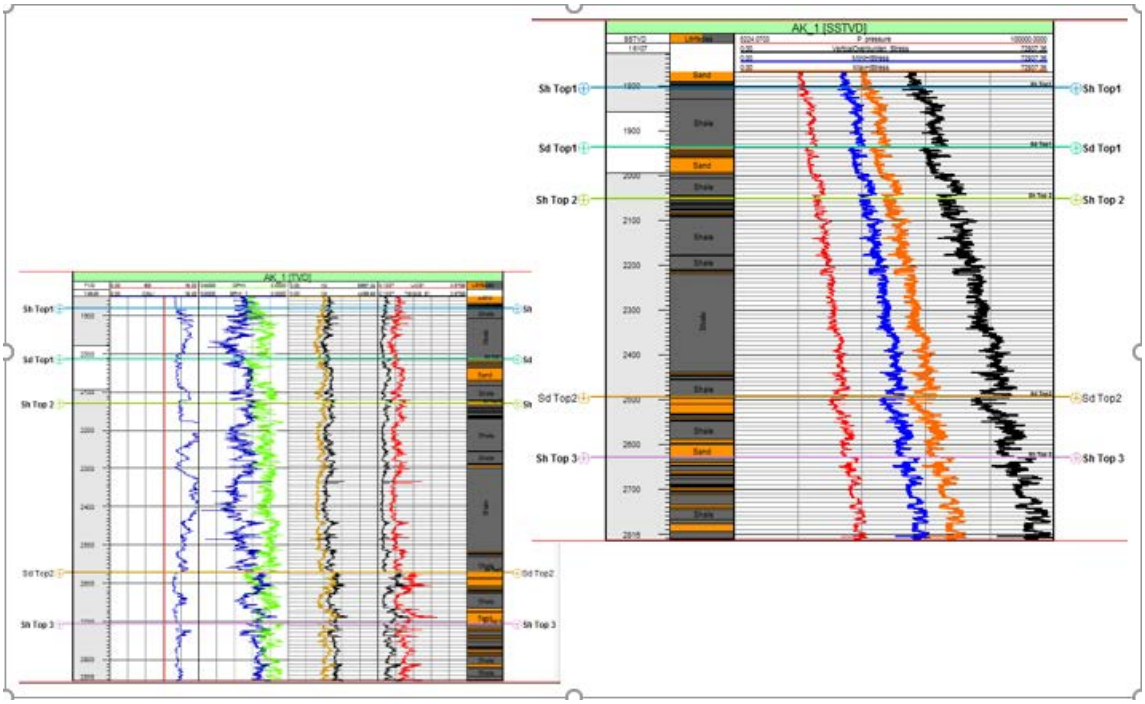


Figure 15: Bit size and caliper, Porosities, unconfined compressional and cohesive strength with Pore pressure and Stress (vertical, and max and mini horizontal) profiles for Ak-1

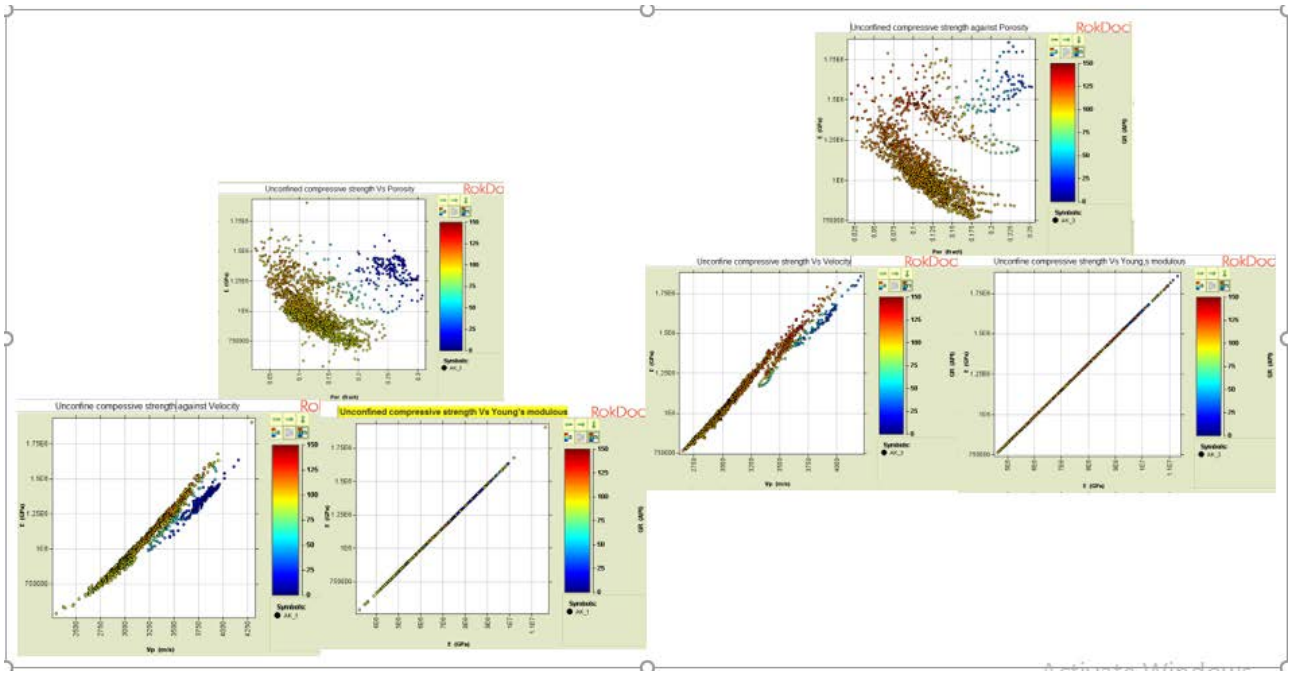


Figure 16: Crossplots of UCS against porosity, velocity and young modulus for AK-1 and 3,

## Conclusion

The geomechanical properties, and rock strength parameters were integrated with all available information from well logs and estimated pore pressure to establish the mechanisms of rock integrity in the study area**.** Mathematical and empirical approach were used to accurately estimate in-situ stress, pore pressures and mechanical parameters using rock properties. The 3D in-situ stress and pore pressure distribution showed an empirical relationship between in-situ stress and density also between the pore pressure and interval transit time which enables the in-situ stress and pore pressure distribution in 3D model following the trend of density and estimated velocity. The results of 3D in-situ stress and rock mechanical models imaged the in-situ stress, elastic and inelastic properties of surrounding area with limited data to analysis the shale formation failure.

Velocity against young's modulus, UCS against young modulus, porosity and velocity, and cohesive strength against internal friction angle cross-plots enable the proper examination of shale formation strength and it incompetent to withstand stress. It was also confirmed the shale formation stress increases with depth as its strength decreases. So, it will take high strength to prevent failure within this formation from the high stress concentration due to it elastic parameters.

REFERENCES

[1]. **Alkamil, E.H.K., Abbood, H.R., Flori, R.E. and Eckert, A., 2017.** Wellbore Stability Evaluation for Mishrif Formation. Paper Presentation at the SPE Middle East Oil & Gas Show and Conference, Bahrain, pp. 1-15.

[2]. **Avbovbo, A. A., 1978.** Tertiary lithostratigraphy of Niger Delta: *American Association of Petroleum Geologists Bulletin*, vol. 62, pp. 295-300.

[3]. **Babatunde A. Salawu, Reza Sanaee, and Olumayowa Onabanjo (2017**). Rock Compressive Strength: A Correlation from Formation Evaluation Data for the Niger Delta* Search and Discovery Article #30488 (2017) **Posted February 20, 2017

[4]. **Barton, N. R., 1973.** Review of a New Shear Strength Criterion for Rock Joints. Engineering Geology, Vol. 7, pp. 287-332.

[5]. **Biot M. A., 1941.** General theory of three-dimensional consolidation. J Appl Phys 12(1): pp155-164.

[6]. **Biot, M.A., 1962.** Mechanics of deformation and acoustic propagation in porous media. Journal of applied physics, 33(4), pp.1482-1498.

[7]. **Bradley W.B. 1974.** Borehole Failure Part 1: Failure of Inclined Boreholes, Technical Progress Report BRC-EP 18-74-P, Shell Bellaire Research Center, Houston, October 1974

[8]. **Burke, K., 1972.** Longshore drift, submarine canyons, and submarine fans in development of Niger Delta: *American Association of Petroleum Geologists, Bulletin* vol. 56, pp. 1975-1983

[9]. **Chang, C., Zoback M. D., & Khaksar, A., 2006.** Empirical relations between rock strength and physical properties in sedimentary rocks: Journal of Petroleum Science and Engineering, 51, 223–237

[10]. Doust, H., and Omatsola, E., (1990). Niger Delta, in, Edwards, J. D., and Santogrossi, P.A., eds., Divergent/passive Margin Basins, AAPG Memoir 48: Tulsa, American Association of Petroleum Geologists, Bulletin, pp. 239-248.

[11]. **Eaton, B.A. (1975).** The equation for geopressure prediction from well logs. SPE, Paper No. 5544, 11P.

[12]. **Evamy, D.D.J., Haremboure, P., Kamerling, W.A., Knaap, F.Molloy, A. and Rowlands, M.H., 1978.** Hydrocarbon habitat of the Tertiary Niger Delta. *American Association of Petroleum Geologists Bulletin* 62, pp. 1–39.

[13]. **Fidelis A. A. and Akaha C. T., 2016.** Geomechanical Evaluation of an onshore oil field in the Niger Delta, Nigeria. IOSR Journal of Applied Geology and Geophysics (IOSR-JAGG), e-ISSN: 2321–0990, p-ISSN: 2321–0982.Volume 4, Issue 1 Ver. I (Jan. - Feb. 2016), pp. 99-111. www.iosrjournals.org

[14]. **Fjaer, E. Holt, R. M. Horsrud, P. Raaen, A. M. and Risnes, R., 1992.** Petroleum Related Rock Mechanics, 2nd edition, Vol.53, Amsterdam, Elsevier Publications ,1992.

[15]. **Jaeger, J. C., and N. G. W. Cook. 1976.** Fundamentals of Rock Mechanics. Chapman and Hall, London, 585 P.

[16]. **Kingsley Nwozor and Gareth Yardley, 2015.** Overburden Stress Estimation: A New Model for the UK Sector of the Central North Sea. Department of Geology and Petroleum Geology, University of Aberdeen, UK .Email: kknwozor@abdn.ac.uk. AAPG ICE Melbourne, Australia. September 2015

[17]. **Kulke, H., 1995.** Regional Petroleum Geology of the World. Part II: Africa, America, Australia and Antarctica: Berlin, Gebrüder Borntraeger, pp. 143-172.

[18]. **Lehnerand De Ruiter, P.A.C., 1977.** Structural history of Atlantic Margin of Africa: *American Association of Petroleum Geologists Bulletin*, v.61, pp. 961-981.

[19]. **Olowokere Mary T., 2010**. Geostatistical modeling of interval velocity to quantifying hydrocarbon resource in multi-layer reservoir from TMB field, Niger Delta. International Journal of the Physical Sciences Vol. 5(12), pp. 1897–1907.

[20]. **Olowokere M. T. and J. S. Ojo, 2008b**. Application of travel-time inversion in velocity anisotropy estimation for lithology discrimination in some parts of the Niger Delta, Nigerian Journal of Mining and Geology (JMG), Vol. 44, (2) pp. 173-182**.**

[21]. **Olowokere M. T. and J. S. Ojo, 2008c.** Seismic stratigraphy of a part of continental margin, Western Offshore Niger Delta, Nigerian Journal of Mining and Geology (JMG), Vol. 44, (1) pp. 83-94.

[22]. **Short, K.C. and Stauble, A.J., 1967.** Outline geology of the Niger Delta. *American Association of Petroleum Geologists Bulletin* 51, pp. 761–779.

[23]. **Stacher P., 1995.** Present understanding of the Niger Delta hydrocarbon habitat, in: M.N. Oti, G. Postma (Eds.), Geology of Deltas, Balkema, Rotterdam, 1995, pp. 257-268.

[24]. **Whiteman, A., 1982.** Nigeria: Its Petroleum Geology, Resources and Potential: London, Graham and Trotman. 394P.

[25]. **Wyllie, M.R.J., Gregory, A.R. and Gardner, G.H.F., 1956.** Elastic Wave Velocities in heterogeneous and Porous Media, Geophysics, 21 (1), pp. 41-70.

[26]. **Yu, J.H.Y. and Smith, M., 2011.** Carbonate Reservoir Characterization with Rock Property Invasion for Edwards Reef Complex, the 73rd EAGE Conference and Exhibition incorporating SPE Europe, 23 -26 May, Vienna, Austria, 346-350.

[27]. **Zhang John J. and Laurence R. Bentley 2005.** Factors determining Poisson's ratio. CREWES Research Report — Volume 17 (2005)

[28]. **Zhang L, Cao P, and Radha KC., 2010.** Evaluation of rock strength criteria for wellbore stability analysis. Int J Rock Mech Min Sci.;47: pp. 1304–1316.

[29]. **Zoback MD et al., 2003.** Determination of stress orientation and magnitude in deep wells. Int J Rock Mech Min Sci 40:pp. 1049-1076.